

Subwavelength nondiffracting beams in multilayered media

C.J. Zapata-Rodríguez · J.J. Miret

Received: 8 January 2010 / Accepted: 3 December 2010 / Published online: 5 January 2011
© Springer-Verlag 2011

Abstract We present a family of p-polarized optical beams that are highly localized around the optical axis and are sustained in a layered medium. This medium is comprised of a stack of thin films made of a material exhibiting negative permittivity, regularly placed in a dielectric host. We exploit the excitation of surface plasmon polaritons leading to enhanced localization near the optical axis. Also we perform an appropriate correction of the 2D wavefront in the vicinity of the beam axis for a perfect phase matching showing an optimal concentration of light.

1 Introduction

Tightly confinement of light has been a motive of interest in the scientific community during decades. In this context we include the Bessel beams [1], a family of optical wavefields with the ability of suppressing the spreading effect associated with diffraction thus being transversally localized around its axial *focus*. They are interpreted as a suitable superposition of plane waves all having a wavevector that projected onto the optical beam axis (OBA) gives the characteristic propagation constant β . This sort of solutions may be found also in stratified media if the vector normal to the interfaces lies along the OBA leading to normal incidence of the beam. However, they cannot be supported with out-of-plane excitation [2].

On the other hand, assuming that the medium is periodic, the elements of any wave superposition are necessarily Bloch modes. Provided the projection β of the pseudomomentum along a direction perpendicular to the periodicity of the medium coincides for all Bloch components, we can construct a localized diffraction-free beam if, additionally, a phase-matching condition is satisfied [3].

In this work we identify some 1D layered structures that can sustain nondiffracting wavefields propagated along the OBA with transversal beamsizes clearly surpassing the diffraction limit. This subwavelength effect is due to two different mechanisms, the existence of photonic bandgaps and the formation of surface resonances in the metal-dielectric interfaces. The excitation of such surface plasmons polaritons (SPPs) are attained at comparatively high values of β , however, leading to a subwavelength beam size.

2 Diffraction-free beams in 1D layered media

Let us consider a monochromatic nondiffracting beam propagating in a 1D lossless periodic structure consisting of alternating layers of negative- and positive-permittivity materials as shown in Fig. 1(a). The y axis is set such that it is perpendicular to the separating surfaces. The period is $L = d_d + d_m$, where d_d and d_m are the thicknesses of the dielectric and *metallic* layers. We also assume that beam propagation is directed along the z axis, so that we may cast the electromagnetic fields as

$$\begin{aligned} \mathbf{E}(x, y, z, t) &= \mathbf{e}(x, y) \exp(i\beta z - i\omega t) \\ \mathbf{H}(x, y, z, t) &= \mathbf{h}(x, y) \exp(i\beta z - i\omega t) \end{aligned} \quad (1)$$

ω being the frequency of the monochromatic radiation. The homogeneity of the wave field in the coordinate z is explicitly parametrized in terms of the propagation constant β . We

C.J. Zapata-Rodríguez (✉)
Departamento de Óptica, Universidad de Valencia, Valencia,
Spain
e-mail: carlos.zapata@uv.es

J.J. Miret
Departamento de Óptica, Farmacología y Anatomía, Universidad
de Alicante, Alicante, Spain

consider TM waves, where \mathbf{H} is in the plane XZ , and, therefore, \mathbf{h}_y vanishes.

The Maxwell equations provide some relations between the transverse fields \mathbf{e} and \mathbf{h} . The electric field \mathbf{e} may be derived from \mathbf{h} by means of the equation $\nabla \times \mathbf{H} = -i\omega\epsilon_0\epsilon\mathbf{E}$, where $\epsilon(y)$ is the relative dielectric constant of the foliar structure, and the relation between the magnetic components can be obtained from the equation $\nabla(\mu_0\mathbf{H}) = 0$. Thus h_x is the scalar wave field from which we may describe the non-diffracting beam unambiguously.

According to the Bloch theorem the modes in a multilayer periodic medium are Bloch waves, which for our stratified medium are of the form

$$h_K(y) \exp(iKy) \exp(ik_{\parallel}\mathbf{R}) \tag{2}$$

where $h_K(y + L) = h_K(y)$ is a periodic function, $\mathbf{k}_{\parallel} = (k_x, \beta)$ is the wave vector onto a plane parallel to the interfaces, $\mathbf{R} = (x, z)$, and K is the Bloch wave number. The function $h_K(y)$ may be written as

$$h_K(y) = \begin{cases} a_m(K) \exp[i(k_{ym} - K)y] \\ \quad + b_m(K) \exp[-i(k_{ym} + K)y] \\ 0 \leq y < d_m \\ a_d(K) \exp[i(k_{yd} - K)y] \\ \quad + b_d(K) \exp[-i(k_{yd} + K)y] \\ d_m \leq y < L \end{cases} \tag{3}$$

the amplitudes a_{α} and b_{α} are constants where $\alpha = m$ refers to the medium of negative dielectric constant (NDC), and $\alpha = d$ stands for the dielectric, and $k_{y\alpha} = \sqrt{(\omega/c)^2\epsilon_{\alpha} - |\mathbf{k}_{\parallel}|^2}$. The relationship between a_{α} and b_{α} can be found by enforcing the boundary conditions and its values by normalization. Therefore, using a matrix method [4] we may obtain in a rather simple way the dispersion equation

$$\cos(KL) = \cos[k_{yd}d_d] \cos[k_{ym}d_m] - \frac{(k_{ym}^2\epsilon_d^2 + k_{yd}^2\epsilon_m^2)}{2k_{yd}k_{ym}\epsilon_d\epsilon_m} \sin[k_{yd}d_d] \sin[k_{ym}d_m] \tag{4}$$

The existence of the Bloch modes requires that $-1 \leq \cos(KL) \leq 1$, i.e. K is real. In Fig. 1(b) we plot the real-valued K solutions of (4) for the multilayer medium we have selected. It is composed of thin metallic films of width $d_m = 50$ nm embedded in a dielectric medium of $\epsilon_d = 2.25$. The period is $L = 450$ nm, and we consider a conductor that at a frequency $\omega = 3.4 \text{ fs}^{-1}$ (wavelength $\lambda_0 = 550$ nm in vacuum) has $\epsilon_m \approx -15$ (similar to its value for silver but neglecting losses). There are three allowed bands ($\text{Im}(K) = 0$). Interestingly two of those bands appear for values $|\mathbf{k}_{\parallel}| > \sqrt{\epsilon_d}(\omega/c)$ (red line in Fig. 1(b)), range where the wavefields are of evanescent nature in the layers. These

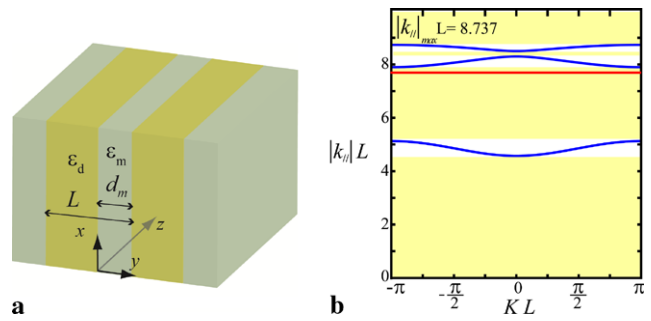


Fig. 1 (a) Schematic geometry of the planar nanolayer-based medium. (b) Dispersion relation for the periodic media chosen ($\omega = 3.4 \times 10^{15}$ rad/s). The regions in yellow denote the bandgaps. The red line marks the boundary between the homogeneous-wave regime and evanescent-wave regime in the dielectric

propagating Bloch modes are a consequence of resonant tunneling of the evanescent waves and possess features of both surface plasmon and Bloch waves.

Returning to our principal objective, we obtain a diffraction-free beam as an adequate superposition of Bloch modes. In particular, the propagating wavefield H_x is constructed as

$$H_x(x, y, z) = \exp(i\beta z) h_x(x, y) = \exp(i\beta z) \sum_K \int_{-\infty}^{\infty} w_K h_K(y) \exp(iKy) \times \exp(ik_x x) dk_x \tag{5}$$

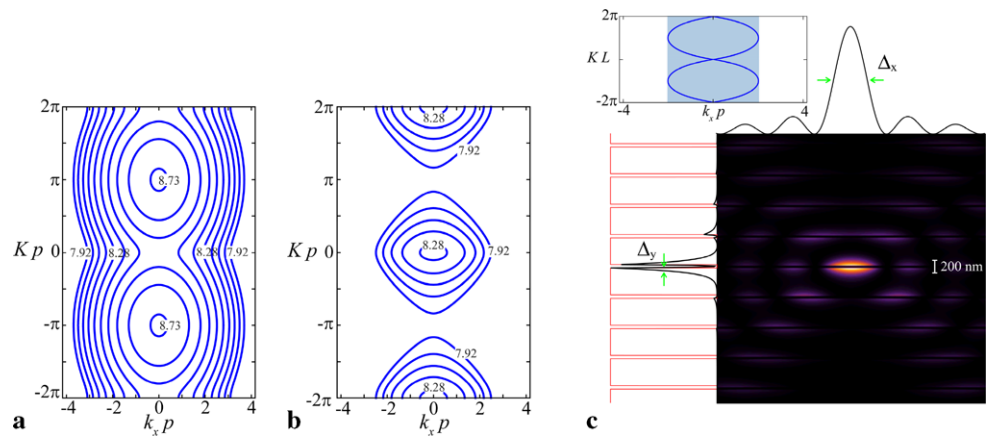
where w_K is simply the weight for the different Bloch modes in the superposition. Keeping in mind that we only consider propagating Bloch modes, we set $w_k = 0$ if $\text{Im}(K) \neq 0$.

We point out that given the propagation constant β , not only the pseudomomentum K but also the spatial frequency k_x is bandlimited. Accordingly, we can generate different non-diffractive waves superposing the Bloch modes belonging to one band or to different bands. In Fig. 2(a) and 2(b) we map different contours of isofrequency β in the $k_x K$ plane for the first and second allowed bands, respectively.

3 Focus generation and results

Only superposing Bloch modes in the form proposed in (5) is not enough to generate a localized beam. We need to establish some favorable conditions for the formation of a focus along the z axis. An advantageous point is the normalization of the periodic function h_K , so we chose $h_K(0) = 1$. In this way using $(x, y) = (0, 0)$ in (5) we obtain the wavefield amplitude $h_x = \sum_K \int_{-\infty}^{\infty} w_K dk_x$ at the origin as a summation of the amplitudes w_K corresponding to different Bloch modes. This may be interpreted as an interfer-

Fig. 2 (a) and (b) Isofrequency curves at different propagation constants β in the first and second sheet of the dispersion curve, respectively. (c) Transverse intensity $|h_x|^2(x, y)$ corresponding to a localized diffraction-free beam of normalized propagation constant $\beta L = 8.503$. Intensity distributions along the coordinate axes are shown at the top and left sides. Inset: Isofrequency curve where the shaded region corresponds to the excited spatial bandwidth



ence of Bloch-type individuals. If the phase of their amplitudes is manipulated in order to have the same value leading to in-phase waves, the oscillatory superposition yields the highest intensity achievable. Moreover, under general conditions it cannot be found a point other than the origin from the xy plane where such a phase matching holds. As a consequence, a strong localization of the nondiffracting beam is expected to occur around the origin, such a point unquestionably constituting a focus. Finally we chose $w_K = 1/\sqrt{|\mathbf{k}_{\parallel}|^2 - (k_x^2 + \beta^2)}$, a form approaching the spectral strength that can be experimental attained, among others, using an opaque screen with a centered extremely thin transparent annulus placed at the front focal plane of a perfect lens [5].

To illustrate the focus generation along the z axis, we perform different numerical simulations for various propagation constants. In Fig. 2(b) we show the field intensity $|h_x|^2$ for a nondiffracting beam of propagation constant corresponding to the lower limit of the first band ($\beta L = 8.503$). The iso-frequency curve is also depicted, where excited frequencies are shaded in grey. The FWHM of the intensity peak along the x axis is $\Delta_x = 505$ nm, which is above the wavelength in the dielectric medium ($\lambda_d = 367$ nm). However, the behavior along the ordinate is significantly different. The wavefield is highly localized in the interfaces of the slabs, leading to fast decays when moving away from the surfaces and thus forming wedge-like shapes. Although the highest peak is attained at $y = 0$, a large one also arises at the other side of the NDC film, $y = d_m$. Ignoring this sidelobe, the FWHM of the figure is $\Delta_y = 61.58$ nm, well below λ_d . In the previous example we have used only the first allowed band. Now fixing the value of β as corresponding to the lower limit of the second band ($\beta L = 7.899$) we may excite every allowed spatial frequency in the evanescent-wave regime of the two highest bands. In this case (Fig. 3(a)) the FWHM along the x axis is $\Delta_x = 277$ nm, lower than λ_d and, more importantly, the high sidelobe appearing previously in the y axis seems to be wiped out completely. This effect may

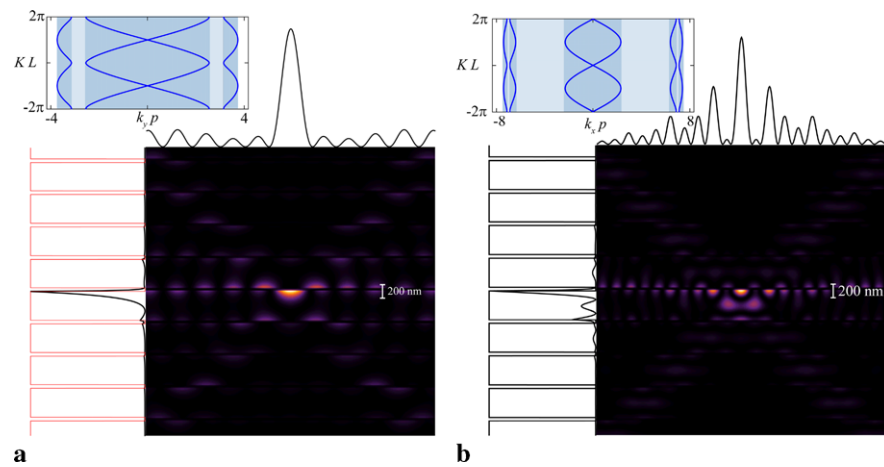
be explained considering that Bloch components from the first band and those from the second band are roughly out of phase at $y = d_m$ so that they interfere destructively in (5). Additionally, the FWHM is $\Delta_y = 54$ nm.

In the simulations given above we have shown that beam-sizes along the x axis are larger than the diffraction limit $\lambda_d/2$ attained by quasi-stationary Bessel beams propagating in the medium of dielectric constant ϵ_d , whereas Δ_y is clearly a subwavelength width. Control over the wave pattern and thus over its FWHM in the x direction is exercised by the spectrum of spatial frequencies k_x : the higher bandwidth the lower Δ_x . In our last illustration we select β coinciding with the lower limit of k_{\parallel} for the third band. We can see the results in Fig. 3(b). A narrow peak on the focus is produced exhibiting a width $\Delta_x = 132$ nm. Also strong sidelobes arise in the vicinity of focus. The presence of two bandgaps explains these effects. The field distribution in the y axis demonstrates a subwavelength focus of FWHM $\Delta_y = 44$ nm. Sidelobes on the interfaces are accompanied by other peaks in the middle of the dielectric slabs. This is not surprising since Bloch components of the third band contributing in the expansion (5) have such a behavior.

4 Conclusions

We have demonstrated that diffraction-free beams propagating in structured media composed of alternating layers of positive and negative ϵ may reach beamsizes surpassing the diffraction limit. In the layered system, two different mechanisms lead to the superresolving effect. A bandpass filtering due to the existence of gaps in the spatial spectrum of k_x modifies the response of the system transversally providing a narrow peak along the x axis with moderate gain ($\Delta_x < \lambda_d/2$) and high sidelobes (secondary foci). In the direction of the periodicity, however, superresolution is carried out by the formation of surface resonances leading to fast decays out of the interfaces. In our numerical simulations, Δ_y

Fig. 3 Transverse intensity $|h_x|^2(x, y)$ for diffraction-free beams of normalized propagation constant (a) $\beta L = 7.899$, and (b) $\beta L = 4.571$. In this last case all three bands of allowed frequencies are excited



may be as low as a third of $\lambda_d/2$. Additionally, dephase of Bloch constituents belonging to different bands contributes to the growth control of secondary foci in nearby surfaces.

Acknowledgements This research was funded by Ministerio de Ciencia e Innovación (MICIIN) under the project TEC2009-11635.

References

1. H.E. Hernández-Figueroa, M. Zamboni-Rached, E. Recami, *Localized Waves* (Wiley, New Jersey, 2008)
2. S. Longhi, D. Janner, P. Laporta, Propagating pulsed Bessel beams in periodic media. *J. Opt. B* **6**(11), 477–481 (2004)
3. J.J. Miret, C.J. Zapata-Rodríguez, Diffraction-free beams with elliptic Bessel envelope in periodic media. *J. Opt. Soc. Am. B* **25**(1), 1–6 (2008)
4. Y. Pochi, *Optical Waves in Layered Media* (Wiley-Interscience, New Jersey, 2005)
5. G. Indebetouw, Nondiffracting optical fields: some remarks on their analysis and synthesis. *J. Opt. Soc. Am. A*, **6**(1), 150–152 (1989)